Electronic Supplementary Material (ESI)

Improved thermoelectric properties of WS_2-WSe_2 phononic crystals: insights from first-principles calculations

Dan Han,[a] Xiaoheng Yang,[a] Mu Du,[b] Gongming Xin,[c] Jingchao Zhang,[d] Xinyu Wang*[a,e] and Lin Cheng*[f]

[a] Institute of Thermal Science and Technology, Shandong University, Jinan 250061, Shandong Province, China

[b] Institute for Advanced Technology, Shandong University, Jinan 250061, Shandong Province, China

[c] School of Energy and Power Engineering, Shandong University, Jinan 250061, Shandong Province, China

[d] NVIDIA Corporation, Santa Clara, CA 95051, USA

[e] Shenzhen Research Institute of Shandong University, Shenzhen 518057, Guangdong Province, China

[f] Shandong Institute of Advanced Technology, Jinan 250100, Shandong Province, China

Corresponding authors. Lin Cheng, Email: cheng@sdu.edu.cn; Xinyu Wang, Email: xyw@sdu.edu.cn.

1. The calculated results of electron relaxation times in all superlattices and their individual components at 300 K

Table S1. The calculated results of the deformation potential constant (E_1), the in-plane elastic modulus (C_{2D}), the effective mass (m*), the carrier mobility (μ_{2D}), and the electron relaxation time (τ_{2D}) of electrons (e) and holes (h) in WS_2, WSe_2, SL1, and SL2 monolayers along the x and y directions at 300 K.

		direction	E_1 (eV)	C_{2D} (J m^{-2})	m^*/m_e	μ_{2D} (cm^2 V^{-1} S^{-1})	τ_{2D} (fs)
WS_2	e	x	7.17	139.35	1.13	82.50	52.98
		y	7.22	139.62	0.34	269.26	52.43
	h	x	1.81	139.35	2.83	276.11	445.03
		y	1.84	139.62	0.48	1592.30	430.62
WSe_2	e	x	6.57	115.93	1.34	59.41	45.33
		y	6.72	116.18	0.39	196.80	43.36
	h	x	1.82	115.93	5.27	84.78	254.15
		y	1.84	116.18	0.53	815.87	247.59
SL1	e	x	6.28	125.09	1.24	72.48	51.21
		y	4.63	128.09	0.46	369.72	96.20
	h	x	1.92	125.09	2.82	204.56	328.89
		y	1.85	128.09	0.56	1145.24	362.53
SL2	e	x	7.30	125.84	1.27	56.26	40.81
		y	6.67	127.91	0.39	225.89	49.77
	h	x	1.93	125.84	7.00	53.29	212.43
		y	1.95	127.91	0.54	638.35	211.16

2. Detailed information about deformation potential constants of all superlattices and their individual components

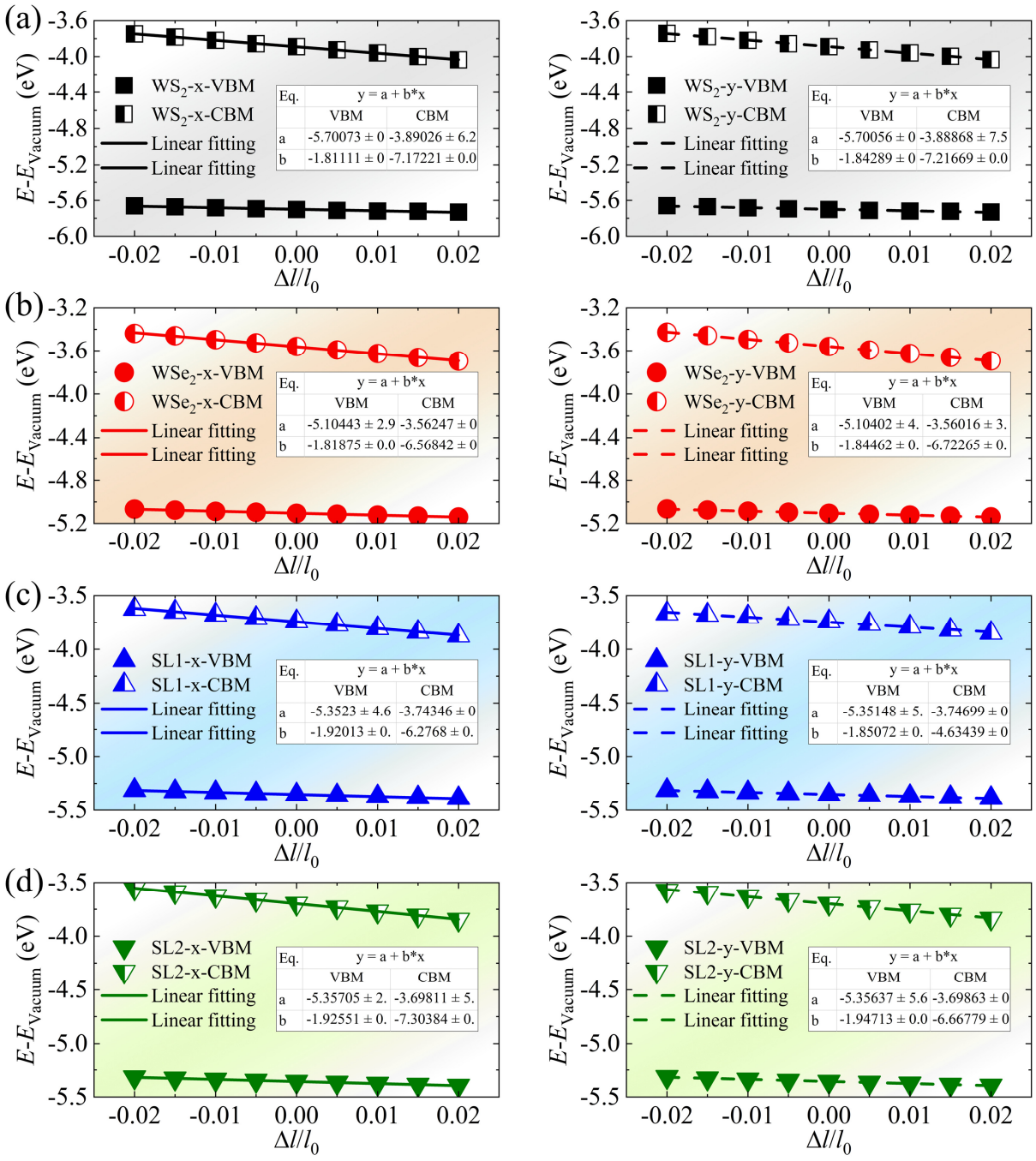

Figure S1. The variations of VBM and CBM of (a) WS_2, (b) WSe_2, (c) SL1, and (d) SL2 monolayers under different strains along the *x* and *y* directions.

3. Detailed information about elastic moduli of all superlattices and their individual components

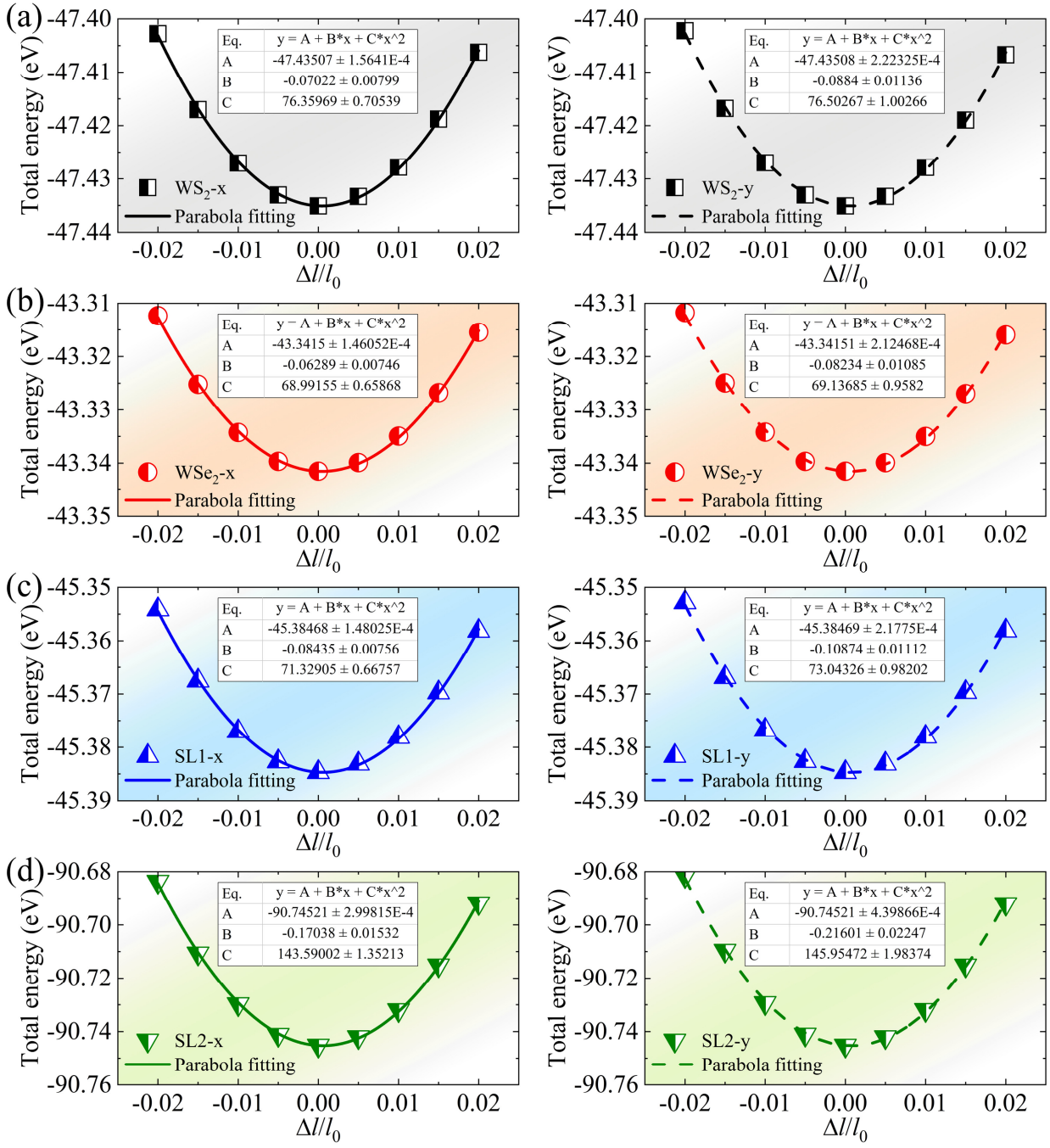

Figure S2. The variations of total energies of (a) WS_2, (b) WSe_2, (c) SL1, and (d) SL2 monolayers under different strains along the *x* and *y* directions.

4. The electronic thermal conductivities obtained from two different formulas of all superlattices and their individual components at 300 K

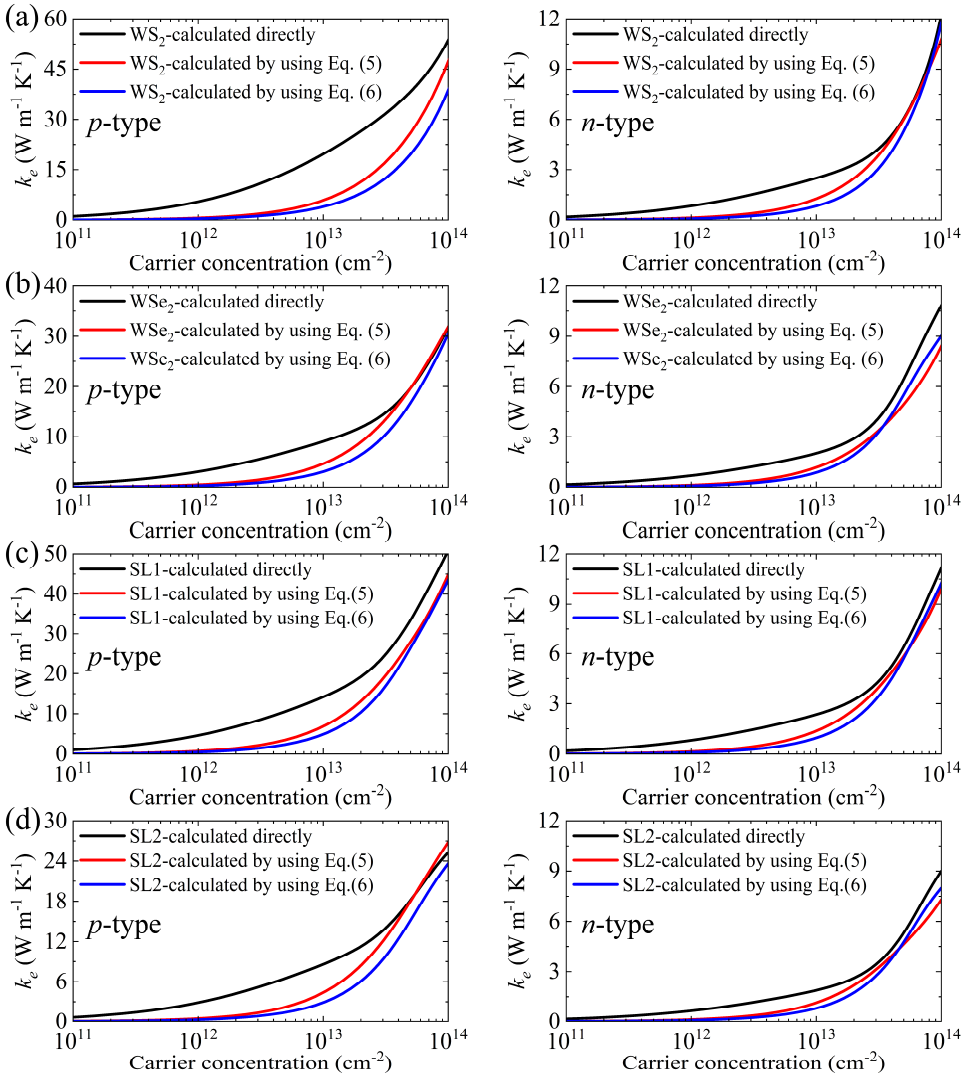

Figure S3. The electronic thermal conductivities (k_e) obtained from Eq. (5) and Eq. (6) of (a) WS_2, (b) WSe_2, (c) SL1, and (d) SL2 monolayers with *p*-type doping and *n*-type doping as a function of the carrier concentration only along the *x* direction at 300 K.

5. The top views of PCH structures

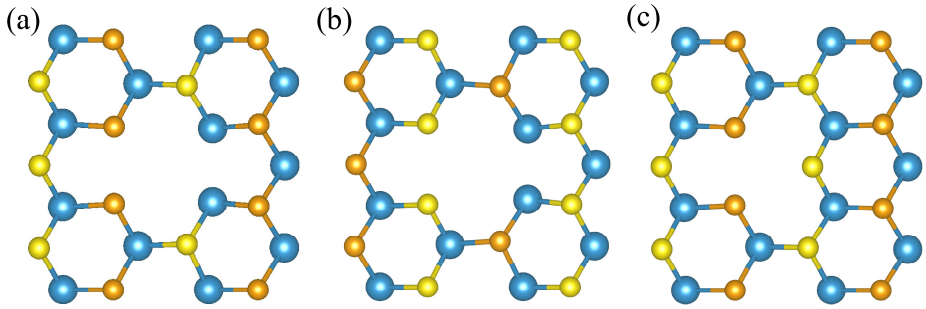

Figure S4. The top views of WS_2-WSe_2 phononic crystals with periodic holes of (a) 1W+2S atoms (PCH3), (b) 1W+2Se atoms (PCH4), and (c) 1W atom (PCH5), respectively.

6. The phonon dispersion curves of all PCH structures

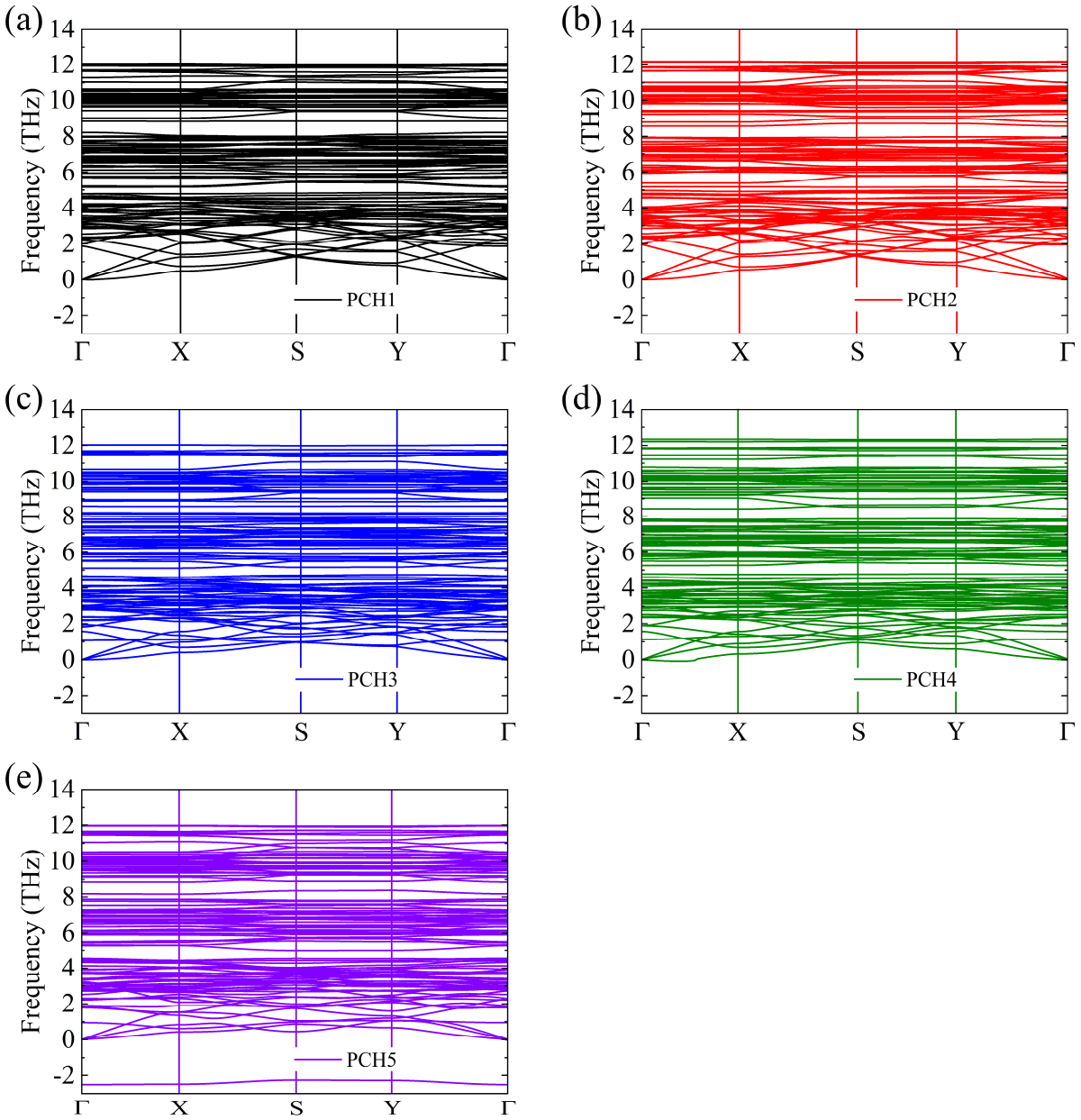

Figure S5. The phonon dispersion curves of (a) PCH1, (b) PCH2, (c) PCH3, (d) PCH4, and (e) PCH5 structures.

7. The average lattice thermal conductivities of four PCH structures

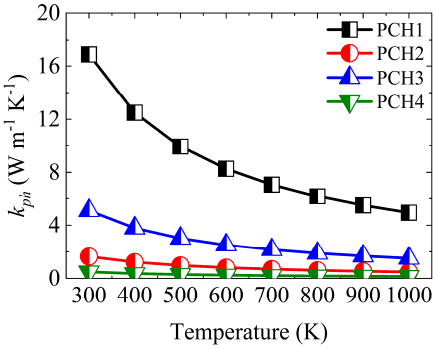

Figure S6. The average lattice thermal conductivities (k_{ph}) of PCH1, PCH2, PCH3, and PCH4 structures as a function of the temperature.

8. The electronic band structures of four PCH structures

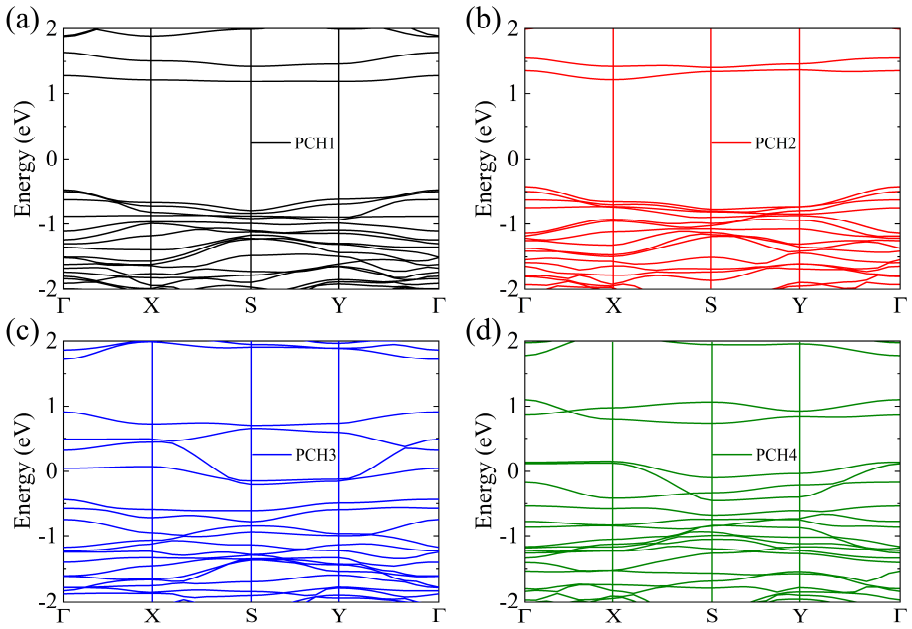

Figure S7. The electronic band structures of (a) PCH1, (b) PCH2, (c) PCH3, and (d) PCH4 structures only employing the HSE06 hybrid functional.